

Rogue waves in the Davey-Stewartson I equation

Yasuhiro Ohta^{1,*} and Jianke Yang^{2,†}¹*Department of Mathematics, Kobe University, Rokko, Kobe 657-8501, Japan*²*Department of Mathematics and Statistics, University of Vermont, Burlington, Vermont 05401, USA*

(Received 15 May 2012; published 17 September 2012)

General rogue waves in the Davey-Stewartson-I equation are derived by the bilinear method. It is shown that the simplest (fundamental) rogue waves are line rogue waves which arise from the constant background with a line profile and then disappear into the constant background again. It is also shown that multirogue waves describe the interaction of several fundamental rogue waves. These multirogue waves also arise from the constant background and then decay back to it, but in the intermediate times, interesting curvy wave patterns appear. However, higher-order rogue waves exhibit different dynamics. Specifically, only part of the wave structure in the higher-order rogue waves rises from the constant background and then retreats back to it, and this transient wave possesses patterns such as parabolas. But the other part of the wave structure comes from the far distance as a localized lump, which decelerates to the near field and interacts with the transient rogue wave, and is then reflected back and accelerates to the large distance again.

DOI: [10.1103/PhysRevE.86.036604](https://doi.org/10.1103/PhysRevE.86.036604)

PACS number(s): 05.45.Yv

I. INTRODUCTION

Rogue waves are large and spontaneous ocean surface waves that occur in the sea and are a threat even to large ships and ocean liners [1]. Recently, an optical analog of rogue waves, optical rogue waves, was also observed in optical fibers [2,3]. A growing consensus is that both oceanic and optical rogue waves appear as a result of modulation instability of monochromatic nonlinear waves. Mathematically, the first and simplest rogue-wave solution was reported in the nonlinear Schrödinger (NLS) equation by Peregrine [4]. This solution approaches a nonzero constant background as time goes to $\pm\infty$ but develops a localized hump with a peak amplitude three times the constant background in the intermediate times. Recently, higher-order rogue waves in the NLS equation were reported in many articles [5–12]. It was shown that these higher-order waves could reach higher peak amplitudes or exhibit multiple intensity peaks at different spatial locations and times. In addition to the NLS equation, rogue waves in some other wave equations (such as the Hirota equation) have also been explored [13]. Rogue waves are intimately related to homoclinic solutions which approach a constant background as time goes to $\pm\infty$ but develop spatially periodic wave patterns in the intermediate times [14–17]. Indeed, rogue waves can be obtained from homoclinic solutions when the spatial period of homoclinic solutions goes to infinity [8,14,15,18].

Rogue waves which have been studied so far are mostly one dimensional, but ocean surface waves are always two dimensional. Thus a natural question is to investigate rogue waves in two-dimensional model equations. It is well known that the evolution of a two-dimensional wave packet on water of finite depth is governed by the Benney-Roskes-Davey-Stewartson equation [19–21]. In the shallow water limit, this equation is integrable (see Ref. [21] and the references therein). This integrable equation is sometimes just called the Davey-Stewartson (DS) equation in the literature. The DS equation

is divided into two types, DSI and DSII equations, depending on the strength of surface tension [21]. The simplest (one-mode) homoclinic solution to the DS equation was derived in Ref. [22]. Taking the spatial period of this homoclinic solution to go to infinity, the simplest (fundamental) rogue-wave solution was also obtained there. But more general rogue waves in the DS equation are still unknown.

In this paper, general rogue waves in the DSI equation are derived. These solutions are obtained by the bilinear method and expressed in terms of determinants. It is shown that the simplest (fundamental) rogue waves are line rogue waves which arise from the constant background with a line profile and then disappear into the constant background again (this simplest rogue wave agrees with that reported in Ref. [22]). It is also shown that nonfundamental rogue waves contain different types such as the multirogue waves and higher-order rogue waves. The multirogue waves describe the interaction of several fundamental rogue waves. These multirogue waves arise from the constant background and then decay back into it, but in the intermediate times, interesting curvy wave patterns appear. Higher-order rogue waves, on the other hand, exhibit certain features which are very different. Specifically, only parts of the wave structures in these higher-order rogue waves rise from the constant background and then retreat back to it, exhibiting unusual transient wave patterns (such as parabola shapes) in the intermediate times. But the other parts of the waves come from the far distance as localized lumps, which interact with the transient rogue waves in the near field and then are reflected back to the large distance again. Since the DS equation describes the evolution of two-dimensional water wave packets [19–21], these rogue-wave solutions could have interesting implications for two-dimensional water wave dynamics.

II. RATIONAL SOLUTIONS IN THE DAVEY-STEWARTSON-I EQUATION

The Davey-Stewartson-I (DSI) equation is given by

$$\begin{aligned} iA_t &= A_{xx} + A_{yy} + (\epsilon|A|^2 - 2Q)A, \\ Q_{xx} - Q_{yy} &= \epsilon(|A|^2)_{xx}, \end{aligned} \quad (2.1)$$

*ohta@math.kobe-u.ac.jp

†jyang@math.uvm.edu

where $\epsilon = 1$ or -1 . It is noted that under the variable transformation $Q \rightarrow Q + \epsilon|A|^2$, $x \leftrightarrow y$, and $\epsilon \rightarrow -\epsilon$, this equation is invariant, thus we can fix the sign of ϵ without loss of generality. However, the transformation $Q \rightarrow Q + \epsilon|A|^2$ changes the boundary condition of Q in general, thus we keep ϵ in our analysis. Equation (2.1) is transformed into the bilinear form,

$$\begin{aligned} (D_x^2 + D_y^2 - iD_t)g \cdot f &= 0, \\ (D_x^2 - D_y^2)f \cdot f &= 2\epsilon(f^2 - |g|^2), \end{aligned} \tag{2.2}$$

through the variable transformation,

$$A = \sqrt{2} \frac{g}{f}, \quad Q = \epsilon - (2 \log f)_{xx}, \tag{2.3}$$

where f is a real variable, g is a complex variable, and D is Hirota's bilinear differential operator.

Rogue waves are rational solutions (under certain parameter restrictions). Thus we first present the general rational solutions to the DSI equation in the following theorem. The proof of this theorem is given in the Appendix.

Theorem 1. The DSI equation (2.1) has rational solutions (2.3) with f and g given by $N \times N$ determinants

$$f = \tau_0, \quad g = \tau_1, \tag{2.4}$$

where $\tau_n = \det_{1 \leq i, j \leq N} (m_{ij}^{(n)})$, and the matrix elements are given by either (a)

$$\begin{aligned} m_{ij}^{(n)} &= \sum_{k=0}^{n_i} c_{ik} (p_i \partial_{p_i} + \xi'_i + n)^{n_i-k} \\ &\quad \times \sum_{l=0}^{n_j} \bar{c}_{jl} (\bar{p}_j \partial_{\bar{p}_j} + \bar{\xi}'_j - n)^{n_j-l} \frac{1}{p_i + \bar{p}_j}, \end{aligned} \tag{2.5}$$

$$\xi'_i = \frac{p_i - \epsilon p_i^{-1}}{2} x + \frac{p_i + \epsilon p_i^{-1}}{2} y + \frac{p_i^2 + p_i^{-2}}{\sqrt{-1}} t, \tag{2.6}$$

or (b)

$$m_{ij}^{(n)} = \sum_{\nu=0}^{n_i+n_j} \left(\frac{-1}{p_i + \bar{p}_j} \right)^{\nu+1} (\partial_x + \partial_y)^\nu P_i^{(n)} \overline{P_j^{(-n)}}, \tag{2.7}$$

$$P_i^{(n)} = \sum_{k=0}^{n_i} \hat{c}_{ik} S_{n_i-k}[\xi^{(n)}(p_i)], \tag{2.8}$$

where $S_n(x)$ is the elementary Schur polynomial defined via the generating function

$$\sum_{n=0}^{\infty} S_n(\mathbf{x}) \lambda^n = \exp \left(\sum_{k=1}^{\infty} x_k \lambda^k \right)$$

for $\mathbf{x} = (x_1, x_2, \dots)$,

$$\xi^{(n)}(p) = [\xi_1(p) + n, \xi_2(p), \dots, \xi_k(p) + \delta_{k1}n, \dots],$$

δ_{ij} is the Kronecker delta notation (which is equal to 1 when $i = j$ and zero otherwise),

$$\begin{aligned} \xi_k(p) &= \frac{1}{k!} \left[\frac{p + \epsilon(-1)^k/p}{2} x + \frac{p - \epsilon(-1)^k/p}{2} y \right. \\ &\quad \left. + \frac{2^k p^2 - (-2)^k/p^2}{2\sqrt{-1}} t \right], \end{aligned}$$

and the overbar represents complex conjugation. In (a) and (b), p_i , c_{ik} , and \hat{c}_{ik} are arbitrary complex constants, and n_i is an arbitrary positive integer. These two expressions in (a) and

(b) would yield identical solutions if the constants c_{ik} and \hat{c}_{ik} in them are related by

$$\hat{c}_{ik} = c_{ik}(n_i - k)!, \quad \hat{d}_{jl} = d_{jl}(n_j - l)!$$

Thus below we use the expression in (a). By a scaling of f and g we can normalize $c_{i0} = 1$ without loss of generality, and thus hereafter we set $c_{i0} = 1$. We will also call the above solution as the N -rational solution of order (n_1, n_2, \dots, n_N) . We comment that a more explicit expression for $m_{ij}^{(n)}$ similar to Eq. (2.6) in Ref. [12] can also be obtained, but since that expression is a bit complicated, we omit it in this paper.

The simplest rational solution, namely, 1-rational solution of first order, is given by taking $N = 1$ and $n_1 = 1$,

$$\begin{aligned} f &= \sum_{k=0}^1 c_{1k} (p_1 \partial_{p_1} + \xi'_1)^{1-k} \sum_{l=0}^1 \bar{c}_{1l} (\bar{p}_1 \partial_{\bar{p}_1} + \bar{\xi}'_1)^{1-l} \frac{1}{p_1 + \bar{p}_1} \\ &= (p_1 \partial_{p_1} + \xi'_1 + c_{11})(\bar{p}_1 \partial_{\bar{p}_1} + \bar{\xi}'_1 + \bar{c}_{11}) \frac{1}{p_1 + \bar{p}_1} \\ &= \frac{1}{p_1 + \bar{p}_1} \left[\left(\xi'_1 + c_{11} - \frac{p_1}{p_1 + \bar{p}_1} \right) \left(\bar{\xi}'_1 + \bar{c}_{11} - \frac{\bar{p}_1}{p_1 + \bar{p}_1} \right) \right. \\ &\quad \left. + \frac{p_1 \bar{p}_1}{(p_1 + \bar{p}_1)^2} \right], \\ g &= \sum_{k=0}^1 c_{1k} (p_1 \partial_{p_1} + \xi'_1 + 1)^{1-k} \\ &\quad \times \sum_{l=0}^1 \bar{c}_{1l} (\bar{p}_1 \partial_{\bar{p}_1} + \bar{\xi}'_1 - 1)^{1-l} \frac{1}{p_1 + \bar{p}_1} \\ &= (p_1 \partial_{p_1} + \xi'_1 + 1 + c_{11})(\bar{p}_1 \partial_{\bar{p}_1} + \bar{\xi}'_1 - 1 + \bar{c}_{11}) \frac{1}{p_1 + \bar{p}_1} \\ &= \frac{1}{p_1 + \bar{p}_1} \left[\left(\xi'_1 + 1 + c_{11} - \frac{p_1}{p_1 + \bar{p}_1} \right) \right. \\ &\quad \left. \times \left(\bar{\xi}'_1 - 1 + \bar{c}_{11} - \frac{\bar{p}_1}{p_1 + \bar{p}_1} \right) + \frac{p_1 \bar{p}_1}{(p_1 + \bar{p}_1)^2} \right], \end{aligned}$$

where

$$\xi'_1 = \frac{p_1 - \epsilon p_1^{-1}}{2} x + \frac{p_1 + \epsilon p_1^{-1}}{2} y + \frac{p_1^2 + p_1^{-2}}{i} t,$$

and p_1, c_{11} are arbitrary complex constants. This solution can be rewritten as

$$f = \frac{1}{p_1 + \bar{p}_1} (\xi \bar{\xi} + \Delta), \quad g = \frac{1}{p_1 + \bar{p}_1} [(\xi + 1)(\bar{\xi} - 1) + \Delta],$$

where

$$\xi = ax + by + \omega t + \theta, \quad \Delta = p_1 \bar{p}_1 / (p_1 + \bar{p}_1)^2,$$

and

$$a = (p_1 - \epsilon p_1^{-1})/2, \quad b = (p_1 + \epsilon p_1^{-1})/2,$$

$$\omega = (p_1^2 + p_1^{-2})/i, \quad \theta = c_{11} - p_1/(p_1 + \bar{p}_1).$$

If we separate the real and imaginary parts of a, b, ω , and θ as $a = a_1 + ia_2$, $b = b_1 + ib_2$, $\omega = \omega_1 + i\omega_2$, $\theta = \theta_1 + i\theta_2$,

then

$$A(x, y, t) = \sqrt{2} \left[1 - \frac{2i(a_2 x + b_2 y + \omega_2 t + \theta_2) + 1}{W} \right],$$

where

$$W = (a_1x + b_1y + \omega_1t + \theta_1)^2 + (a_2x + b_2y + \omega_2t + \theta_2)^2 + \Delta.$$

The solution Q can also be written down from Eq. (2.3) and the above f .

This simplest rational solution has three distinctly different dynamical behaviors depending on the parameter value of p_1^2 .

(1) If p_1^2 is not real, then it is easy to see that b/a is not real, hence $b_1/b_2 \neq a_1/a_2$. In this case, along the $[x(t), y(t)]$ trajectory where

$$a_1x + b_1y = -\omega_1t, \quad a_2x + b_2y = -\omega_2t,$$

(A, Q) are constants. In addition, at any given time, $(A, Q) \rightarrow (\sqrt{2}, 1)$ when (x, y) goes to infinity. Thus the solution is a localized soliton moving on a constant background.

(2) If $p_1^2 < 0$, i.e., p_1 is purely imaginary, then a, b , and ω are all imaginary. In this case, the solution is a function of $a_2x + b_2y + \omega_2t$ only, and is thus a line soliton moving on a constant background.

(3) If $p_1^2 > 0$, i.e., p_1 is real, then a, b are real but ω is imaginary. In this case, the solution is also a line wave, but it is not a moving line soliton anymore. As $t \rightarrow \pm\infty$, this line wave goes to a uniform constant background; in the intermediate times, it rises to a higher amplitude. Thus this is a line wave which ‘‘appears from nowhere and disappears with no trace,’’ hence it is a line rogue wave.

From the above analysis, we see that rational solutions (2.4) to the DSI equation become rogue waves when the parameters p_i are real-valued (this fact holds for $N = 1$ as well as for higher N integers). In the next section, we will examine these rogue waves in more detail.

It is noted from the above explicit solution formulas that the parameter c_{11} causes a shift of the origin in the (x, y, t) space. Thus c_{11} can be set to zero by a shift of the (x, y, t) axes. This fact also holds for $N = 1$ as well as for higher N integers in the solution (2.4).

III. ROGUE WAVES IN THE DAVEY-STEWARTSON-I EQUATION

As we have shown above, rational solutions (2.4) in Theorem 1 become rogue waves in the DSI equation when all parameters p_i are required to be real. In this section, we analyze the dynamics of these rogue waves in detail.

A. Fundamental rogue waves

The fundamental rogue waves in the DSI equation are obtained when one takes $N = 1$, $n_1 = 1$, and p_1 real in the rational solution (2.4), and c_{11} is a free complex parameter. After a shift of time and space coordinates, c_{11} can be eliminated and the fundamental rogue waves can be written as

$$A(x, y, t) = \sqrt{2} \left[1 + \frac{8i\Omega t - 4}{1 + (k_1x + k_2y)^2 + 4\Omega^2 t^2} \right], \quad (3.1)$$

$$Q(x, y, t) = 1 - 4\epsilon k_1^2 \frac{1 - (k_1x + k_2y)^2 + 4\Omega^2 t^2}{[1 + (k_1x + k_2y)^2 + 4\Omega^2 t^2]^2}, \quad (3.2)$$

where

$$k_1 = p_1 - \epsilon p_1^{-1}, \quad k_2 = p_1 + \epsilon p_1^{-1}, \quad \Omega = p_1^2 + p_1^{-2}.$$

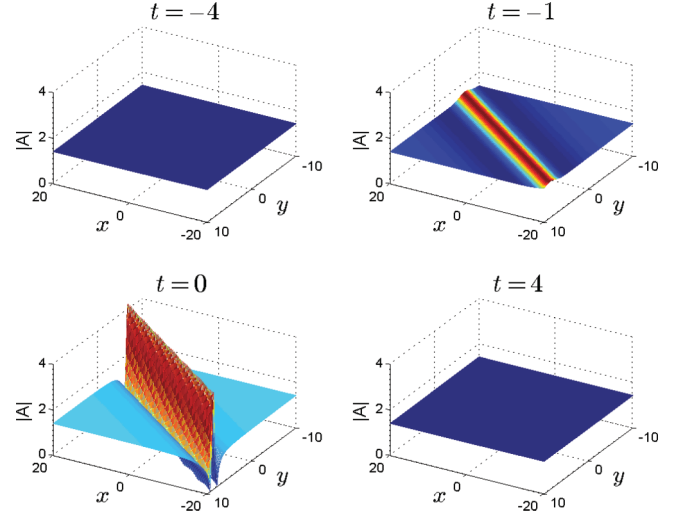


FIG. 1. (Color online) A fundamental rogue wave (3.1) in the DSI equation with parameters $\epsilon = 1$, $p_1 = 1.5$.

This solution describes a line rogue wave with the line oriented in the $(k_2, -k_1)$ direction of the (x, y) plane, thus the fundamental rogue waves in the DSI equation are line rogue waves. The orientation angle β of this line rogue wave is $\beta = -a \tan(k_1/k_2)$, and its width is inversely proportional to $\sqrt{k_1^2 + k_2^2}$. In terms of the orientation angle β , we find that $k_1^2 + k_2^2 = 2(p_1^2 + p_1^{-2}) = 4\epsilon / \cos 2\beta$, thus the width of this line wave is proportional to $\sqrt{\epsilon \cos 2\beta}$, which is angle dependent. Along the line direction (with $k_1x + k_2y$ fixed), the solution is a constant. As $t \rightarrow \pm\infty$, the solution A uniformly approaches the constant background $\sqrt{2}$ everywhere in the (x, y) plane; but in the intermediate times, $|A|$ reaches maximum amplitude $3\sqrt{2}$ (i.e., three times the background amplitude) at the center ($k_1x + k_2y = 0$) of the line wave at time $t = 0$. The speed at which this line wave approaches its peak amplitude is $\Omega = 2\epsilon / \cos 2\beta$, which is also angle dependent. This fundamental rogue wave is illustrated in Fig. 1 with parameters $\epsilon = 1$ and $p_1 = 1.5$.

It is noted that the orientation direction of the line rogue wave (3.1)–(3.2) is not arbitrary due to the above (k_1, k_2) formulas with real p_1 . Indeed, when $\epsilon = 1$, one can see that $|k_1/k_2| < 1$, i.e., the slope of this line wave in the (x, y) plane is always less than one in magnitude. Thus the orientation angle of this line wave is always between -45° and 45° . If $\epsilon = -1$, the situation is opposite. In this case, the orientation angle of the line wave is always between 45° and 135° . These results indicate that for a given ϵ , line rogue waves in the DSI equation have a limited range of orientations.

The above fundamental rogue waves in the DSI equation are two-dimensional counterparts of the fundamental (Peregrine) rogue waves in the NLS equation [4,5]. Indeed, when we take $\epsilon = 1$ and $p_1 = 1$ in the above fundamental rogue waves, we have $k_1 = 0$, hence the solution A is independent of x and $Q = 1$. In this case, the DSI equation reduces to the NLS equation, and this fundamental rogue wave of the DSI equation reduces to the Peregrine rogue wave of the NLS equation.

Nonfundamental rogue waves can be obtained from the N -rational solutions of order (n_1, n_2, \dots, n_N) in Eq. (2.4) with

real values of (p_1, \dots, p_N) when $N > 1$, or $n_1 > 1$, or both. Below we consider two subclasses of these nonfundamental rogue waves.

B. Multirogue waves

One subclass of nonfundamental rogue waves is the multirogue waves, which are obtained when we take $N > 1$, $n_1 = \dots = n_N = 1$ in the rational solution (2.4) with real values of (p_1, \dots, p_N) . These rogue waves describe the interaction of N individual fundamental rogue waves. When $t \rightarrow \pm\infty$, the solution approaches the constant background uniformly in the entire (x, y) plane. In the intermediate times, N line rogue waves arise from the constant background, interact with each other, and then disappear into the background again. In the far field of the (x, y) plane, the solution consists of N separate line rogue waves. However, in the near field where these line rogue waves intersect and interact, wavefronts of the solution are no longer lines, and interesting curvy wave patterns would appear.

To demonstrate these multirogue-wave solutions, we first consider the $N = 2$ case. In this case, the f and g functions of the solutions can be obtained from Eq. (2.4) as

$$f = \begin{vmatrix} m_{11}^0 & m_{12}^0 \\ m_{21}^0 & m_{22}^0 \end{vmatrix}, \quad g = \begin{vmatrix} m_{11}^1 & m_{12}^1 \\ m_{21}^1 & m_{22}^1 \end{vmatrix}, \quad (3.3)$$

where

$$m_{ij}^0 = \frac{1}{p_i + \bar{p}_j} \left[\left(\xi_i' + c_{i1} - \frac{p_i}{p_i + \bar{p}_j} \right) \times \left(\bar{\xi}_j' + \bar{c}_{j1} - \frac{\bar{p}_j}{p_i + \bar{p}_j} \right) + \frac{p_i \bar{p}_j}{(p_i + \bar{p}_j)^2} \right],$$

$$m_{ij}^1 = \frac{1}{p_i + \bar{p}_j} \left[\left(\xi_i' + 1 + c_{i1} - \frac{p_i}{p_i + \bar{p}_j} \right) \times \left(\bar{\xi}_j' - 1 + \bar{c}_{j1} - \frac{\bar{p}_j}{p_i + \bar{p}_j} \right) + \frac{p_i \bar{p}_j}{(p_i + \bar{p}_j)^2} \right],$$

ξ_j' is given by Eq. (2.6), p_1, p_2 are free real parameters, and c_{11}, c_{21} are free complex parameters. The complex parameter c_{11} can be removed by a shift of the (x, y, t) axes, then this two-rogue-wave solution contains four nontrivial real parameters, namely, p_1, p_2 , and the real and imaginary parts of c_{21} . This solution for parameters

$$\epsilon = 1, \quad p_1 = 1, \quad p_2 = 1.5, \quad c_{11} = c_{21} = 0 \quad (3.4)$$

is shown in Fig. 2. It is seen that when these two line rogue waves arise from the constant background, the region of their intersection acquires higher amplitude first (see the $t = -1$ panel). After these higher amplitudes in the intersection region fade, the line rogue solutions in the far field then rise to higher amplitude (see the $t = 0$ panel). Interestingly, the wave pattern at $t = 0$ features two curvy wave fronts which are well separated. These curvy wave fronts are caused by the interaction of the two fundamental (line) rogue waves. At large times, the solution goes back to the constant background again (see the $t = 5$ panel). It is noticed that for all times, the maximum value of the solution $|A|$ does not exceed $4\sqrt{2}$ (i.e., four times the constant background). Thus this interaction

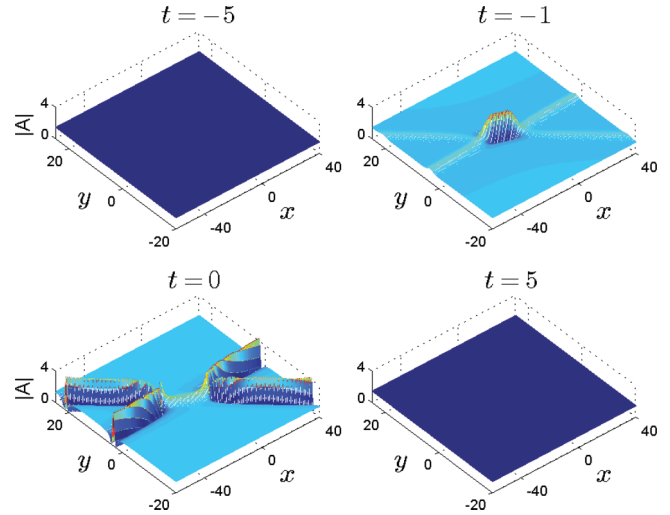


FIG. 2. (Color online) A two-rogue-wave solution (3.3) in the DSI equation for parameters (3.4). Plotted is the $|A|$ field.

between the two line rogue waves does not generate very high peaks.

For larger N , these multirogue waves have qualitatively similar behaviors, except that more line rogue waves will arise and interact with each other, and more complicated wave fronts will form in the interaction region. For example, with $N = 3$ and parameter choices

$$\epsilon = 1, \quad p_1 = 1, \quad p_2 = 1.5, \quad p_3 = 2, \quad (3.5)$$

$$c_{11} = c_{21} = c_{31} = 0,$$

the corresponding solution is shown in Fig. 3. As can be seen, the transient solution patterns become more intricate. But again, the maximum value of this solution $|A|$ stays below $4\sqrt{2}$ for all times, so this interaction does not create very high spikes either.

C. Higher-order rogue waves

Another subclass of nonfundamental rogue waves is the higher-order rogue waves, which are obtained when we take

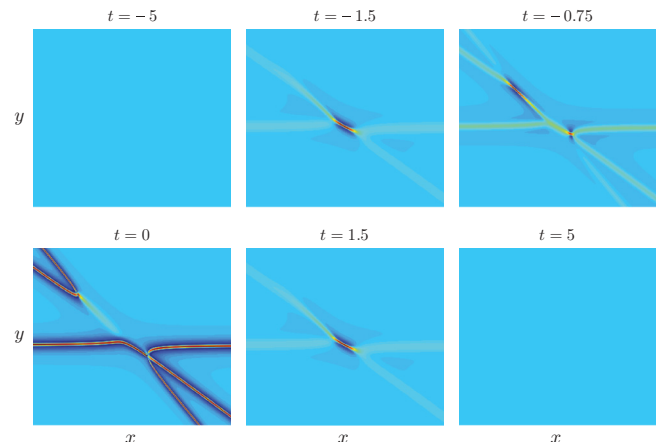


FIG. 3. (Color online) A three-rogue-wave solution in the DSI equation for parameters (3.5). Plotted is the $|A|$ field. The constant-background value is $\sqrt{2}$.

$N = 1$ and $n_1 > 1$ in the rational solution (2.4) with a real value of p_1 . For instance, if $n_1 = 2$, we get second-order rogue waves from Eq. (2.4) as

$$f = [(p_1 \partial_{p_1} + \xi'_1)^2 + c_{12}] \times [(\bar{p}_1 \partial_{\bar{p}_1} + \bar{\xi}'_1)^2 + \bar{c}_{12}] \frac{1}{p_1 + \bar{p}_1}, \quad (3.6)$$

$$g = [(p_1 \partial_{p_1} + \xi'_1 + 1)^2 + c_{12}] \times [(\bar{p}_1 \partial_{\bar{p}_1} + \bar{\xi}'_1 - 1)^2 + \bar{c}_{12}] \frac{1}{p_1 + \bar{p}_1}, \quad (3.7)$$

where ξ'_1 is given by Eq. (2.6), p_1 is a free real parameter, and c_{12} is a free complex parameter. Here we have set $c_{11} = 0$ in Eq. (2.4) by a shift of the (x, y, t) axes. Higher-order rogue waves with $n_1 > 2$ can be similarly obtained.

An interesting phenomenon is that, unlike the multirogue waves discussed above, these higher-order rogue waves do *not* uniformly approach the constant background as $t \rightarrow \pm\infty$. Instead, only parts of their wave structures approach the constant background as $t \rightarrow \pm\infty$, but the other parts move to the far distance as localized lumps with undiminished amplitude and increasing velocity as $t \rightarrow \pm\infty$. To illustrate these behaviors, we consider the above second-order rogue waves. For parameter values

$$\epsilon = 1, \quad p_1 = 1, \quad c_{12} = 0, \quad (3.8)$$

we get

$$f = \frac{1}{2}[x - (4t^2 + y - y^2)]^2 + [(y - \frac{1}{2})^2 + \frac{1}{4}](8t^2 + \frac{1}{2}),$$

$$g = f - 4it(x + y - y^2 - 4t^2) + x + y - y^2 - 12t^2 - \frac{1}{2},$$

and

$$A(x, y, t) = \sqrt{2} \frac{g}{f}. \quad (3.9)$$

For this solution, $\bar{A}(x, y, t) = A(x, y, -t)$, thus $|A(x, y, -t)| = |A(x, y, t)|$. This solution is displayed in Fig. 4. We see that when $|t| \gg 1$, the solution is a localized lump sitting on the constant background $\sqrt{2}$ (see the $t = \pm 7$ panels). The peak

amplitude of the lump is attained at

$$(x, y) = (4t^2 + \frac{1}{4}, \frac{1}{2}),$$

thus this lump is accelerating rightward as $|t|$ increases (see the $t = -7$ and $t = -5$ panels). The peak-amplitude value of the lump stays at $3\sqrt{2}$ and is unchanged though. As the lump accelerates rightward (with increasing $|t|$), its vertical size (along the y direction) remains the same, but its horizontal size (along the x direction) expands (see the $t = -7, -5, -1$ panels). When $t \rightarrow 0$, this lump disappears. At the same time, a parabola-shaped rogue wave rises from the background (see the $t = -1$ and $t = 0$ panels). At $t = 0$, this parabola is located at

$$x = y - y^2,$$

where the rogue wave reaches peak amplitude $3\sqrt{2}$ (see the $t = 0$ panel). Visually one may describe the solution in Fig. 4 as an incoming lump being reflected back by the emergence of a parabola-shaped rogue wave. In addition, this lump decelerates as it comes afar and accelerates as it goes away.

We have also examined the second-order rogue waves (3.6) and (3.7) for other parameter choices of (ϵ, p_1, c_{12}) , and found that those solutions are qualitatively the same as the one in Fig. 4, except that those solution patterns may be stretched and skewed in the (x, y) plane.

IV. SUMMARY

In summary, we have derived general rogue waves in the DSI equation by the bilinear method, and our solutions are given in terms of determinants. We showed that the simplest (fundamental) rogue waves are line rogue waves which arise from the constant background with a line profile and then disappear into the constant background again (see Fig. 1). We also showed that multirogue waves describe the interaction of several fundamental rogue waves, and interesting curvy wave patterns appear due to this interaction (see Figs. 2 and 3). However, higher-order rogue waves were found to show very different features. Specifically, only parts of the wave structures in the higher-order rogue waves rise from the constant background and then retreat back to it, but the other parts of the waves come from the far distance as localized lumps, which interact with the transient rogue waves in the near field and then are reflected back and accelerate to the large distance again (see Fig. 4). These rogue-wave solutions to the DSI equation generalize the rogue waves of the NLS equation into two spatial dimensions, and they could play a role in the physical understanding of rogue water waves in the ocean.

It is noted that for the Benney-Roskes-Davey-Stewartson (BRDS) equations [19,20], some two-dimensional waves bifurcating from a one-dimensional one were constructed in Ref. [23]. Those solutions are different from the solutions in this paper. One difference is that those solutions were derived for the BRDS equations which are elliptic for both variables, and such BRDS equations are not integrable [21]. But in the DSI equation (2.1) studied in this paper, the Q equation is hyperbolic, and this DS system is integrable [21]. Another difference is that the solutions constructed for

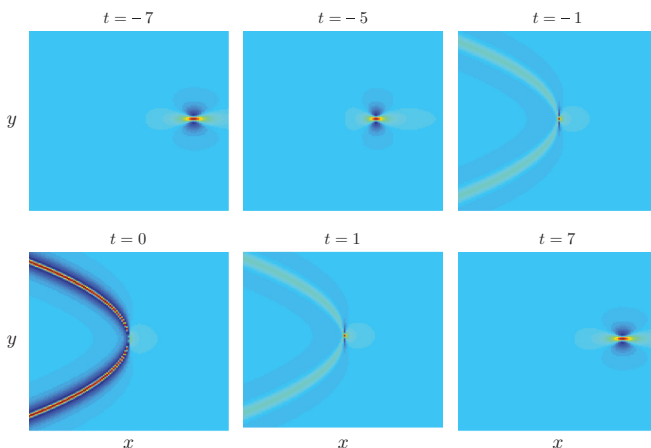


FIG. 4. (Color online) A second-order rogue-wave solution (3.9) in the DSI equation with $\epsilon = 1$.

the BRDS equations in Ref. [23] are time independent, but the rogue-wave solutions derived in this paper for the DSI equation (2.1) are time dependent.

ACKNOWLEDGMENTS

The work of Y.O. is supported in part by JSPS Grant-in-Aid for Scientific Research (B-19340031, S-19104002) and for challenging Exploratory Research (22656026), and the work of J.Y. is supported in part by the Air Force Office of Scientific Research (Grant No. USAF 9550-09-1-0228) and the National Science Foundation (Grant No. DMS-0908167).

APPENDIX

In this Appendix we will prove Theorem 1 in Sec. II by using the bilinear method. First we present the following lemma.

Lemma 1. Let $m_{ij}^{(n)}$, $\varphi_i^{(n)}$, and $\psi_j^{(n)}$ be functions of x_1, x_2, x_{-1} and x_{-2} satisfying the following differential and difference relations,

$$\begin{aligned} \partial_{x_1} m_{ij}^{(n)} &= \varphi_i^{(n)} \psi_j^{(n)}, \\ \partial_{x_2} m_{ij}^{(n)} &= \varphi_i^{(n+1)} \psi_j^{(n)} + \varphi_i^{(n)} \psi_j^{(n-1)}, \\ \partial_{x_{-1}} m_{ij}^{(n)} &= -\varphi_i^{(n-1)} \psi_j^{(n+1)}, \\ \partial_{x_{-2}} m_{ij}^{(n)} &= -\varphi_i^{(n-2)} \psi_j^{(n+1)} - \varphi_i^{(n-1)} \psi_j^{(n+2)}, \\ m_{ij}^{(n+1)} &= m_{ij}^{(n)} + \varphi_i^{(n)} \psi_j^{(n+1)}, \\ \partial_{x_\nu} \varphi_i^{(n)} &= \varphi_i^{(n+\nu)}, \\ \partial_{x_\nu} \psi_j^{(n)} &= -\psi_j^{(n-\nu)} \quad (\nu = 1, 2, -1, -2). \end{aligned} \tag{A1}$$

Then the determinant,

$$\tau_n = \det_{1 \leq i, j \leq N} (m_{ij}^{(n)}), \tag{A2}$$

satisfies the bilinear equations,

$$\begin{aligned} (D_{x_1} D_{x_{-1}} - 2) \tau_n \cdot \tau_n &= -2 \tau_{n+1} \tau_{n-1}, \\ (D_{x_1}^2 - D_{x_2}) \tau_{n+1} \cdot \tau_n &= 0, \\ (D_{x_{-1}}^2 + D_{x_{-2}}) \tau_{n+1} \cdot \tau_n &= 0. \end{aligned} \tag{A3}$$

This lemma can be proved by the same method as for Lemma 3.1 in Ref. [12], thus its proof is omitted here. We note that by the variable transformation

$$x_1 = \frac{1}{2}(x+y), \quad x_{-1} = \frac{\epsilon}{2}(x-y), \quad x_2 = -\frac{i}{2}t, \quad x_{-2} = \frac{i}{2}t, \tag{A4}$$

and the complex conjugate condition

$$\bar{\tau}_n = \tau_{-n}, \tag{A5}$$

the above bilinear equations (A3) are reduced to the bilinear equation (2.2) of the DSI equation for $f = \tau_0$ and $g = \tau_1$. Therefore to prove Theorem 1, all we need to do is to choose appropriate matrix elements $m_{ij}^{(n)}$ which satisfy (A1) and realize the conjugate condition (A5) with (A4).

Proof of Theorem 1. It is easy to see that functions $\varphi_i^{(n)}$, $\psi_j^{(n)}$, and $m_{ij}^{(n)}$ defined by

$$\begin{aligned} \varphi_i^{(n)} &= p_i^n e^{\xi_i}, \quad \psi_j^{(n)} = (-q_j)^{-n} e^{\eta_j}, \\ m_{ij}^{(n)} &= \int^{x_1} \varphi_i^{(n)} \psi_j^{(n)} dx_1 = \frac{1}{p_i + q_j} \left(-\frac{p_i}{q_j} \right)^n e^{\xi_i + \eta_j}, \\ \xi_i &= \frac{1}{p_i^2} x_{-2} + \frac{1}{p_i} x_{-1} + p_i x_1 + p_i^2 x_2, \\ \eta_j &= -\frac{1}{q_j^2} x_{-2} + \frac{1}{q_j} x_{-1} + q_j x_1 - q_j^2 x_2, \end{aligned}$$

satisfy Eqs. (A1). Here p_i, q_j are arbitrary complex constants, and it is assumed that the lower boundary value of the integral in the above $m_{ij}^{(n)}$ equation is zero. But these functions do not lead to rational solutions.

To get rational solutions, we differentiate the above functions with respect to the parameters p_i and q_j . To obtain solution expressions in (a) of Theorem 1, we consider the following $\varphi_i^{(n)}$, $\psi_j^{(n)}$, and $m_{ij}^{(n)}$ functions:

$$\varphi_i^{(n)} = A_i p_i^n e^{\xi_i}, \quad \psi_j^{(n)} = B_j (-q_j)^{-n} e^{\eta_j}, \tag{A6}$$

$$m_{ij}^{(n)} = A_i B_j \frac{1}{p_i + q_j} \left(-\frac{p_i}{q_j} \right)^n e^{\xi_i + \eta_j}, \tag{A7}$$

where A_i and B_j are differential operators of order n_i and n_j with respect to p_i and q_j , respectively, defined as

$$A_i = \sum_{k=0}^{n_i} c_{ik} (p_i \partial_{p_i})^{n_i-k}, \quad B_j = \sum_{l=0}^{n_j} d_{jl} (q_j \partial_{q_j})^{n_j-l}, \tag{A8}$$

c_{ik}, d_{jl} are arbitrary complex constants, and n_i are arbitrary positive integers. It is easy to see that these functions also satisfy Eqs. (A1), thus $\tau_n = \det(m_{ij}^{(n)})$ with (A7) satisfies the bilinear equations (A3). By using the operator relations

$$(p_i \partial_{p_i}) p_i^n e^{\xi_i} = p_i^n e^{\xi_i} (p_i \partial_{p_i} + \xi_i' + n),$$

$$(q_j \partial_{q_j}) (-q_j)^{-n} e^{\eta_j} = (-q_j)^{-n} e^{\eta_j} (q_j \partial_{q_j} + \eta_j' - n),$$

where

$$\begin{aligned} \xi_i' &= -\frac{2}{p_i^2} x_{-2} - \frac{1}{p_i} x_{-1} + p_i x_1 + 2p_i^2 x_2, \\ \eta_j' &= \frac{2}{q_j^2} x_{-2} - \frac{1}{q_j} x_{-1} + q_j x_1 - 2q_j^2 x_2, \end{aligned}$$

the matrix element $m_{ij}^{(n)}$ in Eq. (A7) becomes

$$\begin{aligned} m_{ij}^{(n)} &= \left(-\frac{p_i}{q_j} \right)^n e^{\xi_i + \eta_j} \sum_{k=0}^{n_i} c_{ik} (p_i \partial_{p_i} + \xi_i' + n)^{n_i-k} \\ &\quad \times \sum_{l=0}^{n_j} d_{jl} (q_j \partial_{q_j} + \eta_j' - n)^{n_j-l} \frac{1}{p_i + q_j}. \end{aligned}$$

Taking parameter constraints

$$q_j = \bar{p}_j, \quad d_{jl} = \bar{c}_{jl}, \tag{A9}$$

and using the variable transformation (A4), we obtain

$$\eta_j = \bar{\xi}_j, \quad \overline{m_{ij}^{(n)}} = m_{ji}^{(-n)}, \quad \bar{\tau}_n = \tau_{-n},$$

thus the conjugate condition (A5) is satisfied. Finally using the gauge freedom of τ_n , we obtain the rational solutions to the DSI equation as given in (a) of Theorem 1.

Next we derive solution expressions in (b) of Theorem 1. For this purpose, we consider the following $\varphi_i^{(n)}$, $\psi_j^{(n)}$ and $m_{ij}^{(n)}$ functions:

$$\varphi_i^{(n)} = \hat{A}_i p_i^n e^{\xi_i}, \quad \psi_j^{(n)} = \hat{B}_j (-q_j)^{-n} e^{\eta_j}, \quad (\text{A10})$$

$$m_{ij}^{(n)} = \int^{x_1} \varphi_i^{(n)} \psi_j^{(n)} dx_1, \quad (\text{A11})$$

where \hat{A}_i and \hat{B}_j are differential operators of order n_i and n_j with respect to p_i and q_j defined as

$$\hat{A}_i = \sum_{k=0}^{n_i} \frac{\hat{c}_{ik}}{(n_i - k)!} (p_i \partial_{p_i})^{n_i - k}, \quad (\text{A12})$$

$$\hat{B}_j = \sum_{l=0}^{n_j} \frac{\hat{d}_{jl}}{(n_j - l)!} (q_j \partial_{q_j})^{n_j - l}, \quad (\text{A13})$$

$\hat{c}_{ik}, \hat{d}_{jl}$ are arbitrary complex constants which are related to the constants c_{ik}, d_{jl} in the solution expression (a) as

$$\hat{c}_{ik} = c_{ik}(n_i - k)!, \quad \hat{d}_{jl} = d_{jl}(n_j - l)!,$$

and it is assumed that the lower boundary value of the integral in Eq. (A11) is zero. Rewriting $\varphi_i^{(n)}$ and $\psi_j^{(n)}$ in Eq. (A10) as

$$\hat{A}_i p_i^n e^{\xi_i} = P_i^{(n)} p_i^n e^{\xi_i}, \quad (\text{A14})$$

$$\hat{B}_j (-q_j)^{-n} e^{\eta_j} = Q_j^{(n)} (-q_j)^{-n} e^{\eta_j}, \quad (\text{A15})$$

where $P_i^{(n)}$ and $Q_j^{(n)}$ are polynomials of degrees n_i and n_j in $(x_{-2}, x_{-1}, x_1, x_2)$, respectively, and using integration by parts, $m_{ij}^{(n)}$ in Eq. (A11) then turns into

$$m_{ij}^{(n)} = \left(-\frac{p_i}{q_j} \right)^n e^{\xi_i + \eta_j} \sum_{v=0}^{n_i + n_j} \frac{(-1)^v}{(p_i + q_j)^{v+1}} \partial_{x_1}^v P_i^{(n)} Q_j^{(n)}.$$

Due to the gauge freedom of τ_n , we can see that

$$m_{ij}^{(n)} = \sum_{v=0}^{n_i + n_j} \left(\frac{-1}{p_i + q_j} \right)^{v+1} \partial_{x_1}^v P_i^{(n)} Q_j^{(n)} \quad (\text{A16})$$

gives the same solution. In order for this solution to satisfy the conjugate condition (A5), we take

$$q_j = \bar{p}_j, \quad \hat{d}_{jl} = \bar{c}_{jl}. \quad (\text{A17})$$

Then in view of the variable transformation (A4), we have

$$\overline{Q_j^{(n)}} = P_j^{(-n)}, \quad \overline{m_{ij}^{(n)}} = m_{ji}^{(-n)}, \quad \bar{\tau}_n = \tau_{-n}, \quad (\text{A18})$$

hence τ_n with the above matrix elements (A16) satisfies the bilinear DSI equation (2.2).

Lastly we derive the explicit expression of $P_i^{(n)}$. From the definition of $P_i^{(n)}$ in Eq. (A14), we have

$$\sum_{k=0}^{n_i} \frac{\hat{c}_{ik}}{(n_i - k)!} (p_i \partial_{p_i})^{n_i - k} p_i^n e^{\xi_i} = P_i^{(n)} p_i^n e^{\xi_i}. \quad (\text{A19})$$

For $\xi = \sum_{v=-2,-1,1,2} p^v x_v$, using the functional identity (see the Appendix of Ref. [12])

$$e^{\kappa p \partial_p} F(p) = F(e^\kappa p),$$

we get

$$\begin{aligned} \frac{1}{p^n e^\xi} e^{\kappa p \partial_p} p^n e^\xi &= e^{\kappa n} \exp \left(\sum_v (e^{\nu \kappa} - 1) p^\nu x_\nu \right) \\ &= \exp \left(\kappa n + \sum_{k=1}^{\infty} \frac{\kappa^k}{k!} \sum_v v^k p^\nu x_\nu \right) \\ &= \sum_{k=0}^{\infty} \kappa^k S_k[\xi^{(n)}(p)], \end{aligned} \quad (\text{A20})$$

where $\xi^{(n)}(p) = [\xi_1(p) + n, \xi_2(p), \dots, \xi_k(p) + \delta_{k1}n, \dots]$ and $\xi_k(p) = \sum_v v^k p^\nu x_\nu / k!$. By comparing the coefficient of order κ^k in Eq. (A20), we obtain

$$\frac{1}{p^n e^\xi} (p \partial_p)^k p^n e^\xi = S_k[\xi^{(n)}(p)].$$

Substituting $p = p_i$ and $\xi = \xi_i$ into this equation and inserting it into Eq. (A19), and recalling the variable transformation (A4), we then find the explicit expression for $P_i^{(n)}$ as

$$P_i^{(n)} = \sum_{k=0}^{n_i} \hat{c}_{ik} S_{n_i - k}[\xi^{(n)}(p_i)],$$

where $\xi^{(n)}(p_i)$ is as given in Theorem 1. Inserting this $P_i^{(n)}$ and $Q_j^{(n)}$ from Eq. (A18) into Eq. (A16), the solution expression in (b) of Theorem 1 is then derived. It is noted that by using Lemma 1, we can also directly prove that $m_{ij}^{(n)}$ in the expression (b) of Theorem 1 gives the solution of the bilinear DSI equation (2.2). This ends the proof of Theorem 1.

[1] C. Kharif, E. Pelinovsky, and A. Slunyaev, *Rogue Waves in the Ocean* (Springer, Berlin, 2009).
 [2] D. R. Solli, C. Ropers, P. Koonath and B. Jalali, *Nature (London)* **450**, 1054 (2007).
 [3] B. Kibler, J. Fatome, C. Finot, G. Millot, F. Dias, G. Genty, N. Akhmediev, and J. M. Dudley, *Nat. Phys.* **6**, 790 (2010).
 [4] D. H. Peregrine, *J. Aust. Math. Soc. B* **25**, 16 (1983).
 [5] N. Akhmediev, A. Ankiewicz, and J. M. Soto-Crespo, *Phys. Rev. E* **80**, 026601 (2009).
 [6] P. Dubard, P. Gaillard, C. Klein, and V. B. Matveev, *Eur. Phys. J. Spec. Top.* **185**, 247 (2010).

[7] P. Dubard and V. B. Matveev, *Nat. Hazards Earth. Syst. Sci.* **11**, 667 (2011).
 [8] P. Gaillard, *J. Phys. A* **44**, 435204 (2011).
 [9] A. Ankiewicz, D. J. Kedziora, and N. Akhmediev, *Phys. Lett. A* **375**, 2782 (2011).
 [10] D. J. Kedziora, A. Ankiewicz, and N. Akhmediev, *Phys. Rev. E* **84**, 056611 (2011).
 [11] B. Guo, L. Ling, and Q. P. Liu, *Phys. Rev. E* **85**, 026607 (2012).
 [12] Y. Ohta and J. Yang, *Proc. R. Soc. London, Ser. A* **468**, 1716 (2012).

- [13] A. Ankiewicz, J. M. Soto-Crespo, and N. Akhmediev, *Phys. Rev. E* **81**, 046602 (2010).
- [14] N. Akhmediev, V. M. Eleonskii, and N. E. Kulagin, *Sov. Phys. JETP* **62**, 894 (1985).
- [15] N. Akhmediev, V. M. Eleonskii, and N. E. Kulagin, *Theor. Math. Phys.* **72**, 809 (1988).
- [16] A. R. Its, A. V. Rybin, and M. A. Salle, *Theor. Math. Phys.* **74**, 29 (1988).
- [17] M. J. Ablowitz and B. M. Herbst, *SIAM J. Appl. Math.* **50**, 339 (1990).
- [18] N. Akhmediev, A. Ankiewicz, and M. Taki, *Phys. Lett. A* **373**, 675 (2009).
- [19] D. J. Benney and G. Roskes, *Stud. Appl. Math.* **48**, 377 (1969).
- [20] A. Davey and K. Stewartson, *Proc. R. Soc. London, Ser. A* **338**, 101 (1974).
- [21] M. J. Ablowitz and H. Segur, *Solitons and the Inverse Scattering Transform* (SIAM, Philadelphia, 1981).
- [22] M. Tajiri and T. Arai, *Phys. Rev. E* **60**, 2297 (1999).
- [23] F. Dias and M. Haragus-Courcelle, *Stud. Appl. Math.* **104**, 91 (2000).